

Synthesis and Bioimaging of Positron-Emitting ^{15}O -Labeled 2-Deoxy-D-glucose of Two-Minute Half-Life

Hideki Yorimitsu,^[a] Yoshihiro Murakami,^[b, c] Hiroyuki Takamatsu,^[c]
Shintaro Nishimura,^[b, c] and Eiichi Nakamura^{*[a]}

Abstract: In positron emission tomography (PET), which exploits the affinity of a radiopharmaceutical for the target organ, a systematic repertoire of oxygen-15-labeled PET tracers is expected to be useful for bioimaging owing to the ubiquity of oxygen atoms in organic compounds. However, because of the 2-min half-life of ^{15}O , the synthesis of complex biologically active ^{15}O -labeled organic molecules has not yet been achieved. A state-of-the-art synthesis now makes available an ^{15}O -

labeled complex organic molecule, 6- ^{15}O -2-deoxy-D-glucose. Ultrarapid radical hydroxylation of 2,6-dideoxy-6-iodo-D-glucose with molecular oxygen labeled with ^{15}O of two-minute half-life provided the target ^{15}O -labeled molecule. The labeling reaction with ^{15}O

Keywords: bioimaging • hydroxylation • positron emission tomography • radical reactions • radiopharmaceuticals

was complete in 1.3 min, and the entire operation time starting from the generation of ^{15}O -containing dioxygen by a cyclotron to the purification of the labeled sugar was 7 min. The labeled sugar accumulated in the metabolically active organs as well as in the bladder of mice and rats. ^{15}O -labeling offers the possibility of repetitive scanning and the use of multiple PET tracers in the same body within a short time, and hence should significantly expand the scope of PET studies of small animals.

Introduction

Positron emission tomography (PET) has attracted increasing attention as an advanced molecular-imaging technology. PET utilizes radioactive tracers labeled with positron-emitting nuclides such as ^{18}F and ^{11}C . The positrons emitted in vivo reacts with neighboring electrons to lead to pair annihilations, which produce couples of gamma rays in opposite directions. The emitted gamma rays are detected with a PET scanner that surrounds the subject to visualize the distribution of the tracers. As a technique that is minimally in-

vasive, PET has gained importance in modern clinical diagnosis. ^{18}F -labeled deoxyglucose (^{18}F FDG) accumulates at metabolically active sites, allowing for tumor detection and the evaluation of cerebral and cardiac functions.^[1] Furthermore, pharmaceutical companies worldwide are starting to utilize PET for pharmacokinetic monitoring of new drug candidates.^[2] In situ imaging of ^{11}C -labeled neuroprotective FK506 highlights the utility of PET technology in drug discovery.^[3]

Methods exist to synthesize ^{18}F -labeled complex organic molecules, as illustrated by the success of ^{18}F FDG-based PET technology; ^{18}F -based PET tracers play key roles in PET bioimaging. However, the development of fundamental new chemistry to synthesize tracers that contain common elements such as carbon, nitrogen, and oxygen instead of fluorine would have a big impact in the field.^[4] ^{15}O is ubiquitous in biologically active compounds, and is therefore an ideal element. The 2-min half-life of the oxygen-15 isotope is much shorter than the half-lives of the commonly used positron-emitting isotopes (^{11}C 20 min, ^{13}N 10 min, and ^{18}F 110 min) and represents a unique merit of the ^{15}O -labeled tracer for biological studies. For instance, its rapid decay will allow repetitive PET measurements, leading to quicker diagnosis by the use of a wider variety of short-lived PET tracers. The short half-life is a drawback too. The 2-min half-life

[a] Dr. H. Yorimitsu,⁺ Prof. Dr. E. Nakamura
Department of Chemistry, The University of Tokyo
Hongo, Bunkyo-ku, Tokyo 113-0033 (Japan)
Fax: (+81)3-5800-6889
E-mail: nakamura@chem.s.u-tokyo.ac.jp

[b] Dr. Y. Murakami, Dr. S. Nishimura
Analysis and Pharmacokinetics Research Laboratories
Astellas Pharma Inc.
5-2-3, Tokodai, Tsukuba, Ibaraki 300-2698 (Japan)

[c] Dr. Y. Murakami, Dr. H. Takamatsu, Dr. S. Nishimura
The Medical and Pharmacological Research Center Foundation
Wo32, Inoyama-cho, Hakui, Ishikawa 925-0613 (Japan)

[⁺] Present Address: Department of Material Chemistry
Kyoto University, Nishikyo, Kyoto 615-8510 (Japan)

of ^{15}O makes the chemical synthesis of its labeled compounds a formidable challenge. Chemists have only several minutes for the synthesis and purification, including the time necessary for generation of ^{15}O from ^{15}N (a few minutes) in a cyclotron and mass transfer from the cyclotron to the chemical laboratory (≈ 1 min) as well as from the chemical to the biological laboratory where the PET imaging is carried out. It is therefore not unreasonable that, since a progress report in 1975 on an attempted synthesis of 1- ^{15}O -2-deoxy-D-glucose from H_2^{15}O made from H_2 and $^{15}\text{O}^{16}\text{O}$ gas,^[5] there has been no further mention of the actual synthesis of ^{15}O -labeled organic molecules other than a synthesis^[6] of 1- ^{15}O -butanol.^[7] The synthesis of ^{15}O -containing complex organic molecules has not yet been achieved.

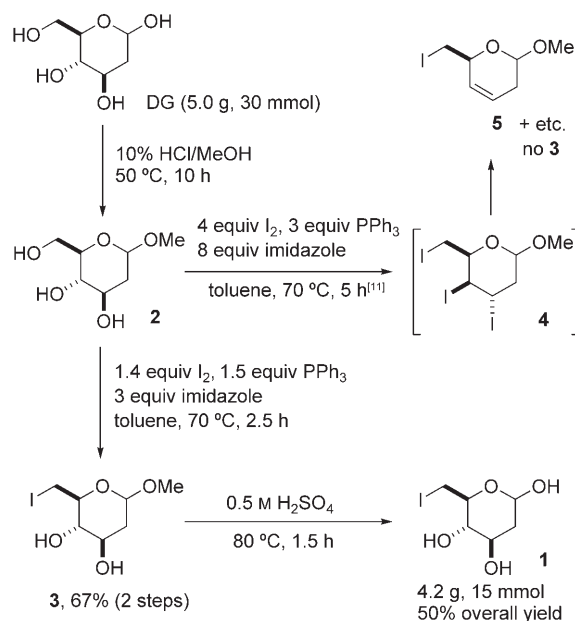
For the synthesis of an ^{15}O -labeled complex organic molecule to be possible and practically useful, it must be exceedingly rapid and clean. In the light of the importance of [^{18}F]FDG in PET, we chose 6- ^{15}O -2-deoxy-D-glucose ([^{15}O]DG) as our first target to establish the feasibility of the required ultrarapid organic synthesis. To this end, we developed some time ago a radical oxygenation reaction of alkyl halides to the corresponding alcohol with air, Bu_3SnH , and a small amount of azobis(isobutyronitrile) (AIBN, radical initiator)^[8] and used it for ^{17}O - and ^{18}O -labeling of complex organic molecules.^[9] These reactions are useful in traditional organic synthesis, but have been found useless in the synthesis of [^{15}O]DG because of slow reaction and low efficiency of oxygen uptake. For the reaction to be useful for ^{15}O -labeling, a number of fundamental problems needed to be resolved: 1) Drastic reduction of the reaction time from over 10 h under air to a few minutes, fighting against the low concentration of the $^{15}\text{O}^{16}\text{O}$ gas supplied from the cyclotron, for instance, as a 1.5:98.5 O_2/N_2 mixture with an $^{15}\text{O}/^{16}\text{O}$ ratio of about 10^{-8} :1, and only as a batch flow of less than 2-min duration instead of a continuous supply; 2) erratic induction time inherent to radical chain reactions, thus requiring careful control of the reaction so that the radical reaction proceeds only during the time when the $^{15}\text{O}^{16}\text{O}$ gas is supplied from the cyclotron; 3) the use of unprotected sugar as a substrate to avoid loss of time in deprotection; 4) enhancement of the reaction selectivity; and 5) a variety

of synthetic and operational issues related to radioactivity and automation. We have overcome these difficulties and developed ultrarapid synthesis and bioimaging of [^{15}O]DG, the details of which are disclosed herein.^[10]

Results and Discussion

Synthesis of Unprotected Iodosugar Precursor

The iodosugar **1** (Scheme 1) that we decided to use as a starting material is a known compound.^[11] The patent literature synthesis of **1** comprises protection of the anomeric hy-



Scheme 1. Preparation of iodosugar **1**.

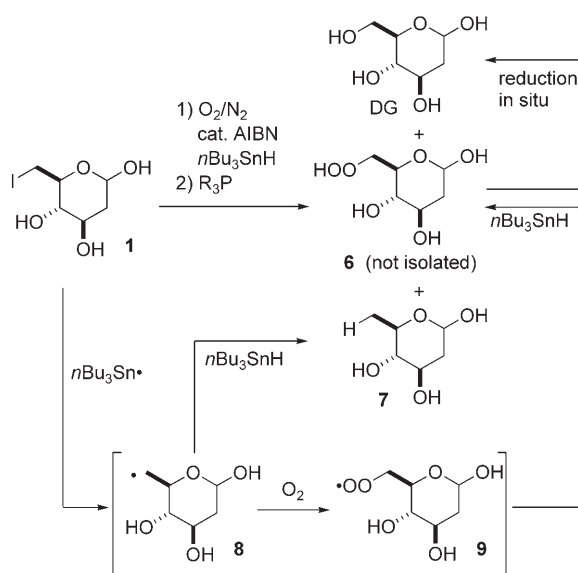
droxy group of 2-deoxy-D-glucose (DG \rightarrow **2**), iodination of the 6-OH group (**2** \rightarrow **3**), and hydrolysis of the anomeric acetal (**3** \rightarrow **1**). Initially, however, we could not reproduce the iodination reaction. A complex mixture containing **5** was obtained instead. We reasoned that the triiodide **4** formed because of the use of excess I_2 (4 equiv), PPh_3 (3 equiv), and imidazole (8 equiv), which gave the olefin **5**. After careful optimization of the conditions, we established a reproducible, large-scale preparation of **1** by reducing the amounts of the iodination agents.^[12] Isolation of **1** was another problem, as it decomposed upon complete removal of water from its aqueous solution at a temperature higher than 40 °C. Careful evaporation of water below 30 °C allowed us to obtain **1** as a white powder.

Radical Hydroxylation Reaction with Cold O_2 in the First-Generation Reaction Vessel

With **1** in hand, we initiated the study to synthesize [^{15}O]DG by the radical-hydroxylation reaction. Scheme 2 outlines our

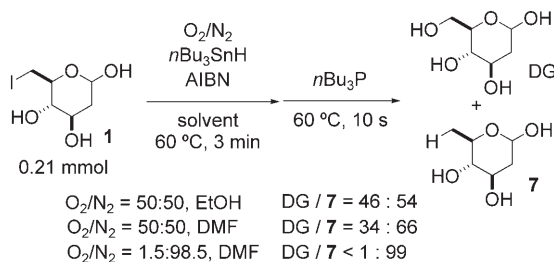
Abstract in Japanese:

陽電子放出断層撮像法(PET)では、体内の特定の場所に親和性を持つ有機化合物を陽電子放出核種でラベルして体内に入れ、その挙動を正確に知ることができる。酸素は有機化合物中に普遍的に存在し、酸素-15は標識核種として理想的である。しかしながらその半減期は2分とあまりに短く、酸素-15標識された複雑な有機化合物は合成できないのではないかと考えられてきた。今回我々は、酸素-15で標識した2-デオキシ-D-グルコースを、6-ヨード-2,6-ジデオキシ-D-グルコースを出発物質として、超高効率ラジカル水酸化反応により一段階で合成した。放射性酸素ガスの導入は1.3分、酸素-15合成用サイクロトロン始動開始から精製完了まで全工程わずか7分である。得られた放射性糖は糖代謝が盛んな臓器に蓄積することを確認し、小動物を用いて陽電子イメージングを達成した。酸素-15標識化合物を用いれば、従来のPETトレーサーでは達成できない短時間での繰り返し測定が可能になり、PETの適用範囲を大きく広げるものと期待できる。

Scheme 2. Mechanism of radical hydroxylation of **1**

working mechanism of the radical hydroxylation of **1** to give [^{15}O]DG. The key steps are 1) rapid generation of radical **8** and 2) efficient capture of **8** with O_2 . An expected by-product is 2,6-dideoxy-D-glucose (**7**) through simple reduction of **8** with $n\text{Bu}_3\text{SnH}$. The hydroperoxide **6** initially formed would be reduced in situ to [^{15}O]DG by the excess $n\text{Bu}_3\text{SnH}$ in the reaction, or by a reducing agent added after the reaction. We needed to avoid borohydride^[8,9] that was used in the original procedure, as sodium borohydride would reduce the masked aldehyde group in DG. Instead, we decided to use milder reducing agents such as triorganophosphine.

The first set of experiments were run with “cold” [^{16}O] O_2 diluted with N_2 (50% v/v) (Scheme 3). On the basis of the



Scheme 3. Reactions in the first-generation reaction vessel. Conditions: O_2/N_2 (200 mL min $^{-1}$), $n\text{Bu}_3\text{SnH}$ (0.43 mmol), AIBN (0.01 mmol), solvent (1.0 mL), 60 °C, 3 min, then $n\text{Bu}_3\text{P}$ (0.60 mmol in 0.50 mL of ethanol), 60 °C, 10 s.

configuration of our homemade automated synthesizer^[13] for “hot” [^{15}O] O_2 experiments, we designed the first-generation vessel shown in Figure 1a. The reactant solution was placed in the inner vessel, and the oxygen gas was introduced from the bottom through a teflon tube ($\phi=0.5$ mm) to trap the oxygen gas efficiently. To dissolve polyhydroxylated **1**, polar solvents such as ethanol and *N,N*-dimethylformamide (DMF) were examined. A higher temperature (e.g., 60 °C, referring to the temperature of the air flow

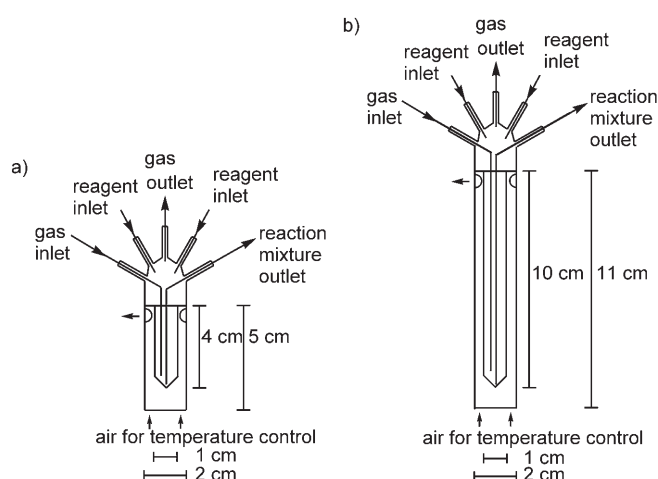


Figure 1. Special reaction vessels for ultrarapid radical hydroxylation made up of two glass tubes of different diameters and teflon tubes. a) First generation, b) second generation. In the cold runs, an oil bath was used for heating instead of warm air.

through the outer tube of the glassware; in the cold experiments, an oil bath was used for heating) was necessary to complete the reaction quickly in a few minutes. The radical oxygenation reactions proceeded with 50% O_2 to afford DG in fair yield. However, the result was disappointing when the reaction was performed with 1.5% O_2 in N_2 , a concentration closer to the one used in the hot experiments. We surmised that the effective concentration of the oxygen gas was too low to oxygenate the radical intermediate in competition with reduction by tin hydride, which existed in large excess.

Radical Hydroxylation with 1.5% O_2/N_2 in the Second-Generation Reaction Vessel

The second-generation reaction vessel was designed (Figure 1b). The vessel is taller than the first-generation reactor and holds a larger amount of solvent. The solvent can retain the oxygen gas more effectively in the reaction medium. We used a mixture of a fluoruous solvent and a polar solvent to dissolve both oxygen and the hydroxy sugar **1**.^[14]

Table 1 summarizes the results of the cold experiments in the new vessel. The sugar **1** (0.2 mmol) was dissolved in a mixture of benzotrifluoride (PhCF_3 ; 7 mL)^[15] and ethanol (1 mL) to obtain a homogeneous solution (Table 1, run 1). The induction period was lengthened to 4 min, as the contents of the larger vessel takes longer to heat. Once the reaction started, however, it was complete in 2 min, and the reaction produced DG in 3% yield. When the concentration was doubled, the yield increased to 10% (Table 1, run 2). Further increase of the concentration improved the yield of DG (Table 1, run 3). In run 3, isopropyl alcohol was used as ethanol tended to be lost during the 10-min reaction time. To enhance the solubility of oxygen gas, a mixture of PhCF_3 and a highly fluorinated perfluorodecaline ($\text{C}_{10}\text{F}_{18}$) was used (Table 1, run 4). The reaction in $\text{PhCF}_3/\text{C}_{10}\text{F}_{18}/i\text{PrOH}$ mixed

Table 1. Reactions in the second-generation reaction vessel.

$1 \xrightarrow[\text{solvent, 60 } ^\circ\text{C, 10 min}]{\begin{matrix} 1.5\% \text{ O}_2/\text{N}_2 \text{ (200 mL min}^{-1}\text{)} \\ n\text{Bu}_3\text{SnH (2 equiv)} \\ \text{AIBN (0.01 mmol)} \end{matrix}} \xrightarrow[\text{60 } ^\circ\text{C, 10 s}]{n\text{Bu}_3\text{P (2 equiv)}} \begin{matrix} \text{HO-CH}_2\text{-CH(OH)-CH}_2\text{-OH} \\ \text{HO-CH}_2\text{-CH(OH)-CH}_2\text{-OH} \\ \text{DG} \end{matrix} + \begin{matrix} \text{HO-CH}_2\text{-CH(OH)-CH}_2\text{-OH} \\ \text{HO-CH}_2\text{-CH(OH)-CH}_2\text{-OH} \\ \text{7} \end{matrix}$

Run	1 [mmol]	Solvent [mL]	DG ^[a] [%], [mmol]	7 ^[a] [%]	1 ^[a] [%]	<i>t</i> ^[b] [min]
1	0.20	PhCF ₃ (7.0) + EtOH (1.0)	3, 0.006	3	94	4–6
2	0.40	PhCF ₃ (7.0) + EtOH (1.0)	10, 0.041	8	76	4–7
3	0.40	PhCF ₃ (3.0) + <i>i</i> PrOH (1.0)	15, 0.059	13	70	4–8
4	0.40	PhCF ₃ (2.0) + C ₁₀ F ₁₈ (1.0) + <i>i</i> PrOH (1.0)	18, 0.071	73	2	3–6

[a] Yields are based on **1**. [b] The time during which the radical propagation reaction was taking place. Reaction time of 4–6 min indicates that the induction for the radical reaction was at 4 min and that the reaction was finished within 6 min of the beginning of the heating of the vessel. In this case, the duration of the radical chain reaction was 2 min. The duration of the radical reaction was determined by TLC monitoring every 1 min.

solvent provided DG in the highest yield of 18% after 3 min accompanied by a large amount of reduction product **7**.

Further optimization on the solvent system was performed (Table 2). Doubling the amount of PhCF₃ shortened the reaction time, although the reaction did not go to completion (Table 2, run 1). Increase in the amount of tin reagent resulted in rapid consumption of the halide but gave less of DG and more of **7** (Table 2, run 2). The choice of alcohol solvent turned out to be important. 2-Butanol is the best alcohol to be used together with the fluorosolvents (Table 2, runs 2–6).

Reactions in the Third-Generation Reaction Vessel Equipped with Sintered-Glass Bottom

To improve the efficiency of oxygen uptake further, we used a sintered-glass gas inlet instead of a teflon tube so that the oxygen gas is introduced as extremely fine bubbles. The third-generation reaction vessel is shown in Figure 2. The new reaction vessel holds 30 mL of solvent. To compensate for the slow warming of the reaction mixture, we used an 80 °C bath in the cold runs. With smaller oxygen gas bubbles and increased solvent volume, the reaction gave DG in 30% yield (Table 3, run 1). As the radical chain propagation lasted for 2.0 min, the yield based on the oxygen gas supplied during the propagation was calculated to be about 50%. Scaling up the reaction improved the oxygen uptake to 70% (Table 3, runs 3 and 4). With efficient oxygen uptake in hand, we started the hot experiments using [¹⁵O]O₂.

Table 2. Reactions in the second-generation reaction vessel.

$1 \xrightarrow[\text{solvent, 60 } ^\circ\text{C, 7 min}]{\begin{matrix} 1.5\% \text{ O}_2/\text{N}_2 \text{ (200 mL min}^{-1}\text{)} \\ n\text{Bu}_3\text{SnH (x mmol)} \\ \text{AIBN (0.01 mmol)} \end{matrix}} \xrightarrow[\text{60 } ^\circ\text{C, 10 s}]{\text{Ph}_3\text{P (1 equiv)}} \begin{matrix} \text{HO-CH}_2\text{-CH(OH)-CH}_2\text{-OH} \\ \text{HO-CH}_2\text{-CH(OH)-CH}_2\text{-OH} \\ \text{DG} \end{matrix} + \begin{matrix} \text{HO-CH}_2\text{-CH(OH)-CH}_2\text{-OH} \\ \text{HO-CH}_2\text{-CH(OH)-CH}_2\text{-OH} \\ \text{7} \end{matrix}$

Run	Tin re-agent [mmol]	Solvent [mL]	DG ^[a] [%], [mmol]	7 ^[a] [%]	1 ^[a] [%]	<i>t</i> ^[b] [min]
1	0.80	PhCF ₃ (4.0) + C ₁₀ F ₁₈ (1.0) + <i>i</i> PrOH (1.0)	18, 0.071	33	49	2–4
2	1.20	PhCF ₃ (4.0) + C ₁₀ F ₁₈ (1.0) + <i>i</i> PrOH (1.0)	15, 0.061	74	5	2–4
3	1.20	PhCF ₃ (4.0) + C ₁₀ F ₁₈ (1.0) + <i>t</i> BuOH (1.0)	11, 0.044	80	5	3–5
4	1.20	PhCF ₃ (4.0) + C ₁₀ F ₁₈ (1.0) + <i>n</i> BuOH (1.0)	6, 0.023	79	0	2–3
5	1.20	PhCF ₃ (4.0) + C ₁₀ F ₁₈ (1.0) + <i>n</i> PrOH (1.0)	11, 0.045	88	0	2–4
6	1.20	PhCF ₃ (4.0) + C ₁₀ F ₁₈ (1.0) + 2-BuOH (1.0)	20, 0.079	63	10	2–4

[a] Yields are based on **1**. [b] See Table 1, footnote [b].

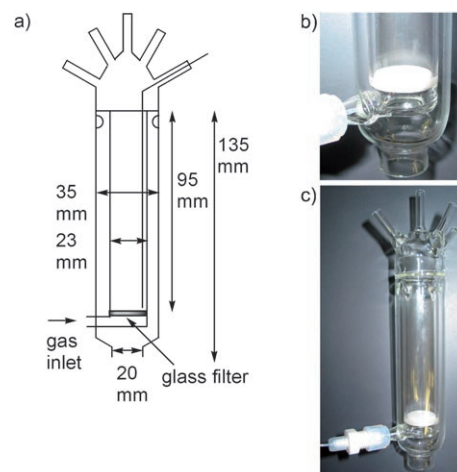


Figure 2. Third-generation reaction vessel. a) Schematic drawing, b) a close-up photo of the sintered-glass bottom, and c) an image of the whole vessel. The internal volume of the vessel is about 0.05 L, 60% of which can hold solvent for the reaction. The reaction vessel has a sintered-glass filter (5–10-μm pore size) as the bottom of the reactor. Oxygen gas was introduced as fine bubbles through the filter to maximize oxygen uptake. The reaction mixture was heated with the aid of the built-in air jacket outside the reaction vessel.

Table 3. Reactions in the third-generation reaction vessel.

$ \begin{array}{c} \text{1} \xrightarrow[\text{solvent, } 80^\circ\text{C, 7 min}]{\begin{array}{l} 1.5\% \text{ O}_2/\text{N}_2 (200 \text{ mL min}^{-1}) \\ n\text{Bu}_3\text{SnH (3.0 equiv)} \\ \text{AIBN (0.025 equiv)} \end{array}} \xrightarrow[\text{80 }^\circ\text{C, 10 s}]{\text{Ph}_3\text{P (1 equiv)}} \text{DG} + \text{7} \end{array} $							
Run	1 [mmol]	PhCF ₃ [mL]	C ₁₀ F ₁₈ [mL]	2-BuOH [mL]	DG [%] ^[a] , [%] ^[b] [mmol]	7 ^[a] [%]	<i>t</i> ^[c] [min]
1	0.40	8.0	1.8	1.2	30, \approx 50, 0.120	54	1.5–3.5
2	0.60	12.0	2.7	1.8	31, \approx 50, 0.182	54	1.5–4.0
3	0.80	16.0	3.6	2.4	28, \approx 70, 0.222	66	1.5–4.0
4	1.00	20.0	4.5	3.0	27, \approx 70, 0.280	71	1.5–4.5

[a] Yield is based on **1**. [b] Yield based on O₂ provided during the reaction period. [c] See Table 1, footnote [b]. The start and end of the reaction were monitored by TLC at 0.5-min intervals.

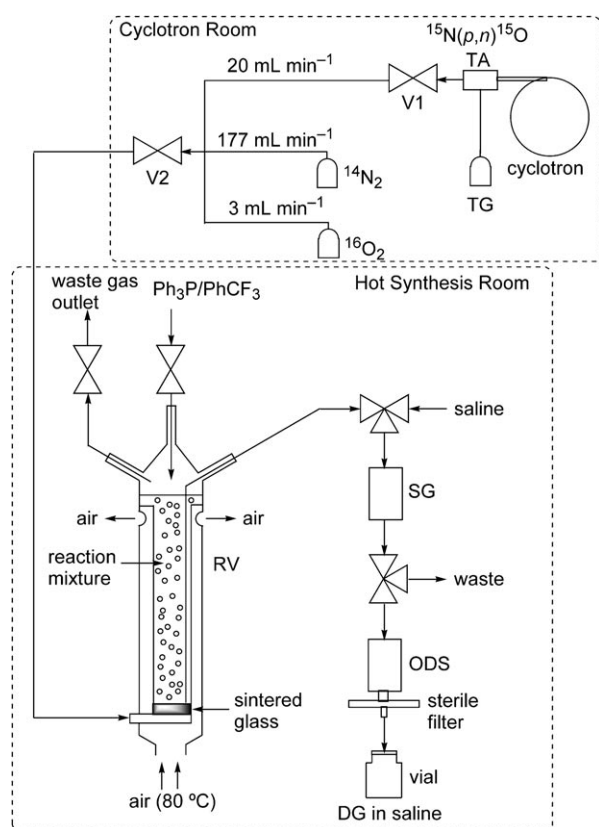


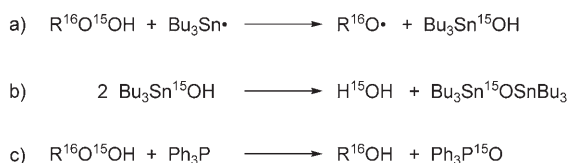
Figure 3. System diagram for [^{15}O]DG synthesis. TA = target area (10 mm ϕ \times 55 mm), TG = target gas cylinder ($^{16}\text{O}_2/^{15}\text{N}_2 = 1.5:98.5$), $^{14}\text{N}_2 = ^{14}\text{N}_2$ gas cylinder, $^{16}\text{O}_2 = ^{16}\text{O}_2$ gas cylinder, RV = the third-generation reaction vessel (Figure 2), SG = Sep-Pak cartridge silica gel Vac 3cc, ODS = two-in-series Sep-Pak cartridges C18 plus short. Valves are shown as triangular assemblies.

Hot Experiments

The synthesis and purification were performed with a fully automated, computer-operated synthesis machine (Figure 3). The details of the experimental procedure are shown below as they are essential to ensure the reproducibility of the labeling experiments. Iodosugar **1** (274 mg, 1.00 mmol) in a

50-mL vial was first dissolved in 2-butanol (3.0 mL) under nitrogen. α, α, α -Trifluorotoluene (20.0 mL), perfluorodecalin (4.5 mL), and AIBN (4.0 mg, 0.025 mmol) were added sequentially to the vial. Tributyltin hydride (807 μL , 3.00 mmol) was introduced with a 100- μL microsyringe with stirring, and the whole homogeneous solution was immediately transferred into the third-generation reaction vessel (RV). The computer-controlled system was set ready for the following synthetic operations: Proton bombardment on target $^{15}\text{N}_2$ gas in the cyclotron in a room next door separated by a 1.5-m-thick concrete wall was started at $t=0$ (valve V1: close). At $t=0.7$ min, supply of both “cold” oxygen gas ($^{14}\text{N}_2 = 177 \text{ mL min}^{-1}$ and $^{16}\text{O}_2 = 3 \text{ mL min}^{-1}$) to the reaction mixture (V2: open) and temperature-controlled air (80°C) to the jacket of RV were started at the same time so that the radical chain reaction could be initiated just when the [^{15}O]O₂ was supplied. The induction time finished at $t=2.2$ min, and the hydroxylation reaction started gradually to generate [^{16}O]DG, peroxide **6**, and 2,6-dideoxy-D-glucose **7**. At $t=4.0$ min, as the chain reaction became faster, the hot gas [^{15}O]O₂/N₂ was released from TA of the cyclotron (20 mL min^{-1} , V1: open), mixed with cold O₂/N₂ gas through V2, and sent to RV in the “hot” synthesis room (200 mL min^{-1}). At $t=4.7$ min, the “hot” gas reached RV. At $t=5.3$ min, the generation of ^{15}O in the cyclotron was stopped, but the gas continued to flow from the cyclotron (V1, V2: open). At $t=6.0$ min, when the increase in radioactivity of RV had nearly stopped, both the “hot” gas and the air at 80°C were stopped (V1, V2: close). At $t=6.1$ min, triphenylphosphine (262 mg, 1.00 mmol in 1.5 mL of PhCF₃) was added to reduce immediately any remaining hydroperoxide **6** to [^{15}O]DG. At $t=6.3$ min, the mixture was passed through SG to retain [^{15}O]DG on the silica gel and to elute most of the tin and phosphine compounds as well as the solvents. The [^{15}O]DG adsorbed was washed out with saline (3 mL), and was then passed through ODS and a sterile filter to trap less-polar compounds in ODS. Thus, we obtained, at $t=7.0$ min, 0.04 mmol of [^{15}O]DG in saline (3 mL). According to HPLC and NMR spectroscopic analysis of cold experiments with the same reagents and setup, this sample was entirely free of tin and phosphine compounds, but contained **7** (0.04 mmol). The dideoxyglucose **7** did not contain ^{15}O and hence did not affect the following PET analysis. The mean radioactivity of the whole solution in a syringe for administration was reproducibly 0.7 GBq at $t=8.0$ min. The decay-corrected radiochemical purity was about 70%, the remainder being ^{15}O -labeled water (see below). The reproducibility depended critically on the duration of the induction period, which could be controlled through careful standardization of the chemical and instrumental details (see Experimental Section).

The solution of [^{15}O]DG in saline was a 7:3 mixture of [^{15}O]DG ($t_R = 4.5$ min; see Experimental Section) and H₂ ^{15}O ($t_R = 2.3$ min). The S_H2 reaction shown in Scheme 4^[16] inevitably formed H₂ ^{15}O via $n\text{Bu}_3\text{Sn}^{15}\text{OH}$. Complete removal of the radioactive water remains a technical problem to be resolved when the present technology goes to a developmental



Scheme 4. Plausible mechanism for the formation of H_2^{15}O , $(\text{Bu}_3\text{Sn})_2^{15}\text{O}$ (a and b), and $^{15}\text{OPPh}_3$ (c).

stage. In this proof-of-principle experiment, H_2^{15}O did not hamper the bioimaging of ^{15}O (see below). Taking into consideration the chemical yield in the cold experiments, the mechanical loss during purification, the generation of 8 GBq of ^{15}O at $t=8.0$ min, and the fact that only half of the ^{15}O in the $^{15}\text{O}^{16}\text{O}$ gas can be incorporated into the sugar molecule (the remainder becomes H_2^{15}O , $^{15}\text{OPPh}_3$, and $(\text{Bu}_3\text{Sn})_2^{15}\text{O}$; Scheme 4), we calculated the yield of ^{15}O (DG) based on ^{15}O to be a very respectable roughly 80% before purification (for detailed calculations, see Experimental Section).

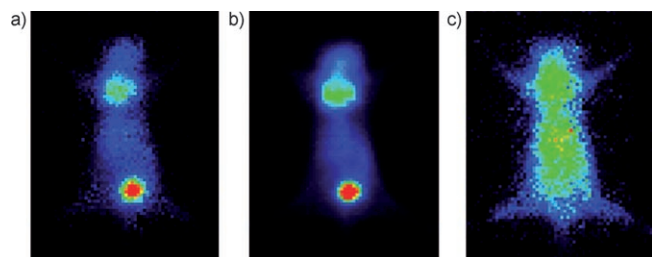


Figure 4. Typical planar positron images of a) ^{15}O (DG), b) ^{18}F (FDG), and c) H_2^{15}O in 6-week-old male mice taken by PPIS. Each image represents the accumulation image from 15 to 30 min after intravenous injection of the tracer into a tail vein. Red pixels indicate highest accumulation of ^{15}O , followed by yellow, green, and blue the lowest. In a) and b), the red and green pixels are located in the bladder and the heart, respectively.

Imaging

A part (0.2 mL) of the solution of ^{15}O (DG) in saline was administered to mice at $t=8.1$ – 8.2 min. Figure 4a shows an image of ^{15}O (DG) in one of the mice obtained by planar positron imaging system (PPIS)^[17] between 15 and 30 min after initiation of the administration. The image is very similar to that obtained with ^{18}F (FDG) (Figure 4b), which reflects the accumulations in the heart and the bladder. The ^{15}O -labeled sugar thus visualized the glucose metabolism in mice. The image completely differed from that visualized by H_2^{15}O (Figure 4c). The dissimilarity assured us that the image in Figure 4a is due to ^{15}O (DG) and not H_2^{15}O , and that the imaging of ^{15}O (DG) was not much affected by the H_2^{15}O in ^{15}O (DG).

Imaging in rats, which are larger than mice, with 3 mL of the solution provided additional accumulations in the brain and the kidneys (Figure 5a). The image is similar to that obtained with ^{18}F (FDG) (Figure 5b).

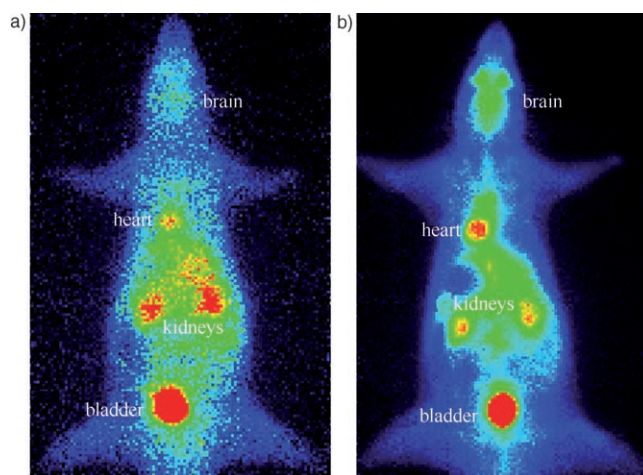


Figure 5. Planar positron images of a) ^{15}O (DG) and b) ^{18}F (FDG) in a 9-week-old male rat.

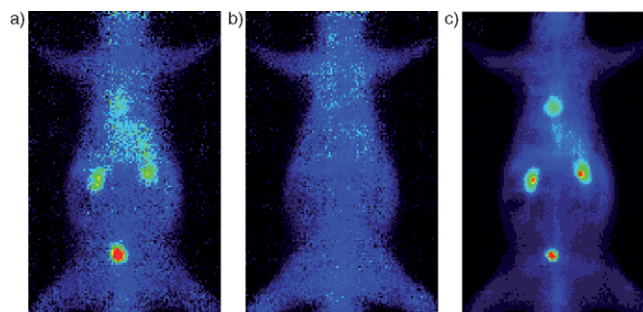


Figure 6. Planar positron images of sequential ^{15}O (DG)– H_2^{15}O – ^{18}F (FDG) measurements (a)–(c), respectively. The PPIS scans were performed similarly.

The advantage of the short half-life of ^{15}O (DG) culminated in sequential ^{15}O (DG)– H_2^{15}O – ^{18}F (FDG) measurements (Figure 6). The three sequential measurements were performed at intervals of five minutes to obtain the images; the whole operation was complete within a few hours. This ^{15}O -labeling will make possible repetitive scanning and the use of multiple PET tracers in the same body over a short period, and hence should significantly expand the scope of experimental protocols in animal PET studies. With these results in hand, we are currently developing new analytical protocols for ^{15}O -based metabolic analysis.^[18]

Conclusions

An exceedingly short-lived ^{15}O -labeled PET tracer as complex as ^{15}O (DG) has been synthesized. The labeled sugar is already useful for in vivo PET imaging in small animals. Thanks to the wide scope and chemoselectivity of the radical hydroxylation reactions in organic synthesis,^[8,9] the present method is applicable to the synthesis of various ^{15}O -labeled PET tracers. The procedure for ^{15}O -labeling is simple,

it involves just the passing of [^{15}O] O_2 through a mixture of tin hydride and a precursor halide compound, which is carried out with a fully automated machine. The whole setup can be made into a robotic ^{15}O -labeling machine. The one-step synthetic operation is much less complicated than ^{11}C -labeling, which requires a multistep operation starting with either ^{11}CO or $^{11}\text{CO}_2$ ^[4,19–21] but enjoys the merits of the much longer half-life of the carbon isotope. The new ^{15}O -labeling technique should promote the development of medicinal and biological investigations with ^{15}O -labeled tracers both in academia and in industry.

The synthesis of structurally complex ^{15}O PET tracers that have a half-life of only 2 min has been a challenge for synthetic chemists in terms of overcoming *time* as a synthetic difficulty. The work herein provides the first solution to the problem that once appeared insurmountable.

Experimental Section

Instrumentation for Cold Experiments

^1H NMR (400 MHz) and ^{13}C NMR (100 MHz) spectra were recorded on a JEOL EX-400 spectrometer in CD_3OD as solvent, and the chemical shift values are reported in δ relative to CD_3OD (3.30 ppm for ^1H NMR and 49.00 ppm for ^{13}C NMR). TLC analyses were performed on commercial glass plates bearing a 0.25-mm layer of Merck silica gel 60F₂₅₄. Elemental analyses were carried out at the Elemental Analysis Center of the University of Tokyo. Flash column chromatography on silica gel 60 (spherical, neutral, 140–325 mesh, Kanto Chemical) was carried out according to the method of Still et al.^[22] The hydroxylation was performed in the reaction vessels shown in Figures 1 and 2. For the cold experiments, an oil bath was used to control the reaction temperature, whereas in the hot experiments, temperature-controlled air was used for heating. O_2/N_2 gas was introduced into the reaction mixtures by a mass-flow system, SEC-400MARKS3 and PAC-S5, obtained from STEC Co. Ltd. For solid-phase extraction to purify sugars quickly, Sep-Pak cartridges (silica, long body) were purchased from Waters and were used after being conditioned with 10 mL of toluene prior to use.

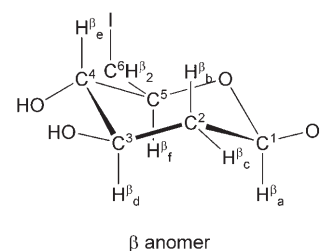
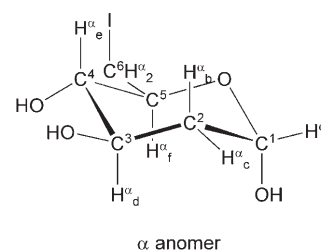
Chemicals

Chemicals and solvents were used as received. 2-Deoxy-D-glucose was purchased from Aldrich. 2-Butanol, α,α,α -trifluorotoluene, and perfluorodecalin were obtained from Kanto Chemical, Acros, and Fluorochem Ltd., respectively. Triphenylphosphine and AIBN were purchased from Wako Pure Chemical. Tributylphosphine was purchased from TCI. $n\text{Bu}_3\text{SnH}$ containing 0.5% 2,6-di-*tert*-butyl-4-methylphenol was obtained from Aldrich (Catalogue No. 23478–8, 10 g). For reproducibility experiments, the Bu_3SnH sample must be used fresh from the bottle. Once kept for more than a few days in a once-opened bottle, the “old” reagent (even after careful distillation) caused low reproducibility of the radical reaction. O_2/N_2 mixed gas was obtained from Takachiho Kagaku Kogyo.

Syntheses

1: 2-Deoxy-D-glucose (5.00 g, 30.0 mmol) was placed in a 100-mL round-bottomed flask equipped with a Dimroth condenser. Hydrochloric acid in methanol (10%, 60 mL) was added to the flask. After being flushed with nitrogen, the mixture was heated at 50°C, and the homogeneous solution was heated at reflux for 10 h. After cooling to ambient temperature, silver(I) carbonate was added with vigorous stirring until generation of carbon dioxide ceased. The mixture was passed through a pad of celite, and the filtrate in a 1000-mL round-bottomed flask was concentrated in vacuo and diluted with toluene (250 mL). The flask was flushed with dry nitrogen, and imidazole (6.12 g, 90.0 mmol), triphenylphosphine (11.8 g, 45.0 mmol), and iodine (11.5 g, 42.0 mmol) were added successively.

After further addition of 200 mL of toluene, the mixture was heated at 70°C for 2.5 h under nitrogen with vigorous stirring using a large stirrer bar. The reaction remained heterogeneous. The toluene layer was transferred to a round-bottomed flask and concentrated. The remaining gummy residue in the reaction flask was triturated with chloroform. The suspension in chloroform was filtrated through celite, and the filtrate was concentrated. The toluene and chloroform extracts were combined and carefully purified by silica-gel chromatography (chloroform/methanol = 20:1). The chromatography fractions contained 5.9 g of 1-*O*-methyl-2,6-dideoxy-6-iodo-D-glucose (20 mmol, 67% yield over two steps). Sulfuric acid (0.5 mol L⁻¹, 200 mL) was added to the purified 1-*O*-methyl-2,6-dideoxy-6-iodo-D-glucose, and the mixture was heated at 80°C with stirring for 1.5 h. A clear solution was obtained as the reaction proceeded. After the mixture was cooled to room temperature, sodium hydrogencarbonate was carefully added portionwise to the acidic solution. Neutralization to pH 7 was checked with indicator paper, and the mixture was then concentrated in vacuo (bath temperature 40°C). Before complete removal of solvent (10–20 mL), methanol (100 mL) was added to the flask to afford a white precipitate (largely Na_2SO_4). Filtration through celite, concentration of the filtrate (bath temperature 30°C), and silica-gel column purification (chloroform/methanol = 8:1) afforded **1** (4.2 g, 15 mmol, 50% overall yield). Pure iodosugar **1**, an amorphous white solid, is unstable at over 40°C and hence must be kept in a refrigerator under inert atmosphere. Spectroscopic data of **1** (mixture of anomers (shown below), α/β =



6:4 in CD_3OD): ^1H NMR (400 MHz, CD_3OD): δ = 1.47 (ddd, J = 10.0, 12.0, 12.4 Hz, 0.4H, H^b_b), 1.58 (ddd, J = 3.6, 11.6, 12.8 Hz, 0.6H, H^b_b), 2.02 (ddd, J = 0.8, 4.8, 12.8 Hz, 0.6H, H^a_c), 2.13 (ddd, J = 2.0, 4.8, 12.4 Hz, 0.4H, H^b_c), 2.99 (ddd, J = 2.4, 6.4, 8.8 Hz, 0.6H, H^a_c), 3.06 (dd, J = 8.8, 8.8 Hz, 0.6H, H^a_c), 3.11 (dd, J = 8.8, 8.8 Hz, 0.4H, H^b_c), 3.35 (dd, J = 6.4, 10.8 Hz, 0.6H, CH^a_2I), 3.38–3.46 (m, 0.8H, CH^b_2I and H^b_f), 3.50–3.61 (m, 1.4H, CH^a_2I , CH^b_2I and H^b_d), 3.90 (ddd, J = 4.8, 8.8, 11.6 Hz, 0.6H, H^a_d), 4.82 (dd, overlapping with CD_3OH , H^b_b), 5.24 ppm (dd, J = 0.8, 3.6 Hz, 0.6H, H^a_a). The coupling constants of H^b_b indicate the existence of two axial protons in comparison with the coupling constants of H^a_b , providing evidence for the assignment of α and β anomers. ^{13}C NMR (100 MHz, CD_3OD): α anomer: δ = 9.16 (C^6), 39.65 (C^2), 69.16 (C^3), 71.65 (C^5), 77.41 (C^4), 92.83 ppm (C^1); β anomer: δ = 7.41 (C^6), 41.92 (C^2), 71.99 (C^3), 76.49 (C^5), 76.71 (C^4), 95.03 ppm (C^1); elemental analysis: calcd (%) for $\text{C}_6\text{H}_{11}\text{IO}_4$: C 26.30, H 4.04; found: C 26.49, H 4.33.

Reaction in Scheme 3: Iodosugar **1** (58.6 mg, 0.213 mmol) and AIBN (1.6 mg, 0.010 mmol) were placed in a 5-mL vial. Ethanol (1.0 mL) was added, and the mixture was sonicated to form a fine suspension. Tributyltin hydride (115 μL , 0.428 mmol) was introduced by a microsyringe. Note that addition by a normal syringe may cause initiation of the reaction before bubbling to give only **7**. The whole mixture was transferred with a Pasteur pipette into the first-generation reaction vessel. The mixture was then immersed in an oil bath (60°C) with bubbling of mixed gas (O_2/N_2 =

50:50, 200 mL min⁻¹). After 3.0 min, tributylphosphine (0.15 mL, 0.60 mmol) in ethanol (0.50 mL) was quickly introduced to the reaction mixture, and further bubbling and heating continued for 10 s. The mixture was drained into a 20-mL round-bottomed flask, and the vessel was rinsed with methanol (3 mL). Concentration followed by ¹H NMR spectroscopic measurement of the crude oil revealed the formation of DG and **7**^[23] in a ratio of 46:54. Silica-gel column purification (chloroform/methanol=8:1) afforded 16.0 mg of DG (0.097 mmol, 46%) and 17.0 mg of **7** (0.114 mmol, 54%).

Reaction in Table 1, run 4: Iodosugar **1** (108 mg, 0.400 mmol) and AIBN (1.6 mg, 0.010 mmol) were placed in a 10-mL vial. Isopropyl alcohol (1.0 mL), benzotrifluoride (2.0 mL), and perfluorodecalin (1.0 mL) were sequentially added. Tributyltin hydride (215 μ L, 0.800 mmol) was introduced by a microsyringe. The homogeneous solution was transferred with a Pasteur pipette into the second-generation reaction vessel. The vessel was then immersed in an oil bath (60°C) with bubbling of mixed gas (O₂/N₂=1.5:98.5, 200 mL min⁻¹). TLC analysis was done every 1 min, which indicated that the reaction actually started at 3 min and was completed at 6 min after the heating started. After 10.0 min, tributylphosphine (0.20 mL, 0.80 mmol) in benzotrifluoride (0.50 mL) was quickly added to the mixture, and further bubbling and heating continued for 10 s. The mixture was discharged into a 20-mL round-bottomed flask, and the reaction vessel was rinsed with methanol (3 mL). Concentration followed by silica-gel column purification (chloroform/methanol=8:1) afforded 0.071 mmol of DG, 0.292 mmol of **7**, and 0.008 mmol of **1** (determined by ¹H NMR, 1,1,2,2-tetrachloroethane as an internal standard).

Reaction in Table 2, run 6: Iodosugar **1** (108 mg, 0.400 mmol) and AIBN (1.6 mg, 0.010 mmol) were placed in a 10-mL vial. 2-Butanol (1.0 mL) was added, and **1** was dissolved. Benzotrifluoride (4.0 mL) and perfluorodecalin (1.0 mL) were then added. Tributyltin hydride (323 μ L, 1.20 mmol) was introduced by a microsyringe. The solution was transferred into the second-generation reaction vessel. The vessel was then heated in an oil bath (60°C) with bubbling of mixed gas (O₂/N₂=1.5:98.5, 200 mL min⁻¹). TLC analysis was done every 1 min, which indicated that the reaction actually started at 2 min and was completed at 4 min after the heating started. After 7.0 min, the reaction mixture was transferred to a solution of triphenylphosphine (105 mg, 0.40 mmol) in benzotrifluoride (0.50 mL). Concentration under reduced pressure afforded a mixture of oil and viscous residue. Toluene (7 mL) was added, and the solution was passed through Sep-Pak Cartridge silica (long body, conditioned with 10 mL of toluene prior to use). Here the gummy residue, which consisted of sugars, was not soluble in toluene. The eluent containing tin and phosphine compounds was removed. Again, toluene was added to the gummy residue, and a toluene layer was passed through the same cartridge. The cartridge was then washed with methanol (2 \times 5 mL) by using the same syringe that was employed to take up the solutions of toluene. The methanol eluent was added to the gummy sugars. Evaporation and ¹H NMR spectroscopic measurement revealed that the mixture consisted of 0.079 mmol (20%) of DG, 0.252 mmol (63%) of **7**, and 0.042 mmol (10%) of **1**, in addition to traces of tin and phosphine impurities.

Reaction in Table 3, run 2: Iodosugar **1** (162 mg, 0.600 mmol) and AIBN (2.4 mg, 0.015 mmol) were dissolved in 2-butanol (1.8 mL) in a 20-mL vial under nitrogen. Benzotrifluoride (12.0 mL) and perfluorodecalin (2.7 mL) were then added. Tributyltin hydride (485 μ L, 1.80 mmol) was introduced by a microsyringe. The homogeneous solution was placed in the third-generation reaction vessel. The reactor was then heated in an oil bath (80°C) with bubbling of 1.5% O₂ in N₂ (200 mL min⁻¹). The sintered glass provided very fine bubbles. TLC analysis was done every 0.5 min, which indicated that the reaction actually started at 1.5 min and was completed at 4.0 min after the heating started. After 7.0 min, the reaction mixture was transferred to a solution of triphenylphosphine (157 mg, 0.600 mmol) in toluene (1.5 mL). The reaction vessel was rinsed with methanol (10 mL) once. After concentration under reduced pressure, toluene (10 mL) was added. The resulting supernatant was passed through a Sep-Pak Cartridge silica (long body, conditioned with 10 mL of toluene prior to use). Toluene (10 mL) was added again to the gummy residue, and the toluene layer was passed through the same cartridge.

The cartridge was then washed out with methanol (2 \times 5 mL). The methanolic eluent was added to the gummy sugars. Evaporation and ¹H NMR spectroscopic analysis revealed that the mixture consisted of 0.182 mmol of DG (31% based on **1**, \approx 50% based on O₂ that passed through the solution during the radical chain) and 0.402 mmol (67%) of **7**, in addition to traces of tin and phosphine impurities.

Instrumentation for Hot Experiments

Production of ¹⁵O was performed with ¹⁵N(*p*, *n*)¹⁵O reaction by proton bombardment (12 MeV, 50 μ A) of a ¹⁵N₂ target containing 1.5% ¹⁶O₂ using a cyclotron-target system (OSCAR-12, NKK/Oxford) at The Medical and Pharmaceutical Research Center Foundation. Typically, 3 \times 10 GBq of crude [¹⁵O]O₂ was obtained at saturation (4.0 min after the beginning of the bombardment). The [¹⁵O]O₂ reached the RV without passing through soda lime and activated charcoal. The automated synthetic apparatus, with which the "hot" syntheses were performed in a lead-shielded hood, was made inhouse by Fujisawa Pharmaceutical Co., Ltd.^[13] The labeling was performed with the synthetic system illustrated in Figure 3. The third-generation reaction vessel (Figure 2) was used for the hot radical hydroxylation. Sep-Pak cartridges, Vac 3cc and plus C18 short, for purification were purchased from Waters. The cartridges Vac 3cc were conditioned with PhCF₃ (10 mL). The cartridges plus C18 short were conditioned with methanol (10 mL) and saline (10 mL). Saline was purchased from Otsuka Pharmaceutical Co., Ltd. Radioactivity was measured with an RI calibrator (Capintec, CRC127R). Radiochemical purity was determined by high-performance liquid chromatography with an Agilent1100 HPLC system (Agilent Technologies Japan, Tokyo) and an Aloka positron detector RLC-700 (Aloka Co., Ltd, Tokyo, Japan) using a high-performance carbohydrate column (4.6 mm \times 250 mm, Waters Corporation, MA, USA) eluted with 15% water/85% acetonitrile at a flow rate of 2.0 mL min⁻¹.

Calculation of the Yield of [¹⁵O]DG Based on [¹⁵O]O₂

The incorporation yield of [¹⁵O]DG based on ¹⁵O was calculated as follows: The mean radioactivity of the saline solution obtained was 0.7 GBq at 8.0 min, 70% of which came from [¹⁵O]DG. Thus the radioactivity of [¹⁵O]DG itself was calculated to be 0.7 GBq \times 70% = 0.49 GBq at 8.0 min. The cold experiment revealed that 0.27 mmol of DG was formed in the reaction flask. Thus, the reaction flask in the hot experiment would have 0.49 GBq \times 0.27 mmol/0.04 mmol = 3.3 GBq of [¹⁵O]DG at 8.0 min. On the other hand, the cyclotron system produced 7.8 GBq of [¹⁵O]O₂ at 8.0 min (3 \times 10 GBq at 4.0 min) under the same conditions. In theory, only half of the ¹⁵O produced is able to be incorporated into [¹⁵O]DG. The theoretical maximum radioactivity of [¹⁵O]DG is thus 3.9 GBq at 8.0 min. Therefore, the incorporation yield of [¹⁵O]DG based on ¹⁵O was calculated to be 3.3 GBq/3.9 GBq \approx 80%.

Positron Imaging with [¹⁵O]DG, H₂¹⁵O, and [¹⁸F]FDG

The studies were performed on 6-week-old male mice with a body weight of about (30 \pm 3) g and on 9-week-old male Wistar rats with a body weight ranging from 192 to 216 g. All animals were housed in a room maintained at (23 \pm 3)°C with (55 \pm 5)% humidity, and with a 12-h light/dark cycle (light on at 07:00 h). The minimum quarantine period was at least 1 week before the experiment. The animals were housed five per cage and allowed free access to food and water. All the experiments were performed in accordance with the institutional guidelines of the Experimental Animal Committee of The Medical and Pharmacological Research Center Foundation.

Each animal was anesthetized with intraperitoneal injection of ethylcarbamide (Wako, Osaka, Japan; 1.0 g kg⁻¹) and fixed on an acrylic plate placed at a central position between the detector units of a PPIS (IPS-1000-6XII, Hamamatsu Photonics, Shizuoka, Japan).^[17]

H₂¹⁵O (0.5 GBq) was prepared with an automated apparatus (JFE corporation, Tokyo, Japan). [¹⁸F]FDG (10 MBq for the rats, 1.0 MBq for the mice) was made according to the conventional method.^[24] [¹⁵O]DG (mean radioactivity: 0.6 GBq/3 mL at *t* = 8.1 min) was intravenously injected manually from a tail vein over 0.4 min (3 mL for the rats) or 0.1 min (0.2 mL for the mice). Five minutes after the beginning of the in-

jection, the animals were scanned with a 5-frame sequence lasting 25 min (five frames, 5 min each). Five minutes after taking the final frame, [^{18}F]FDG was also injected, and the emission scan was similarly performed. The array of [^{15}O]DG, H_2^{15}O , and [^{18}F]FDG measurements was similarly performed.

Acknowledgements

This work was supported by JSPS KAKENHI (S), the 21st century COE Program for Frontiers in Fundamental Chemistry from MEXT (to E.N.) and by KAKENHI for JSPS Fellows (to H.Y.). We thank Dr. Akihiro Noda for help with the PPIS imaging. Dr. Masahiro Yamanaka and Dr. Cecile Savarin are acknowledged for their important earlier contributions.

- [1] a) B. M. Gallagher, A. Ansari, H. Atkins, V. Casella, D. R. Christman, J. S. Fowler, T. Ido, R. R. MacGregor, P. Som, C.-N. Wan, A. P. Wolf, D. E. Kuhl, M. Reivich, *J. Nucl. Med.* **1977**, *18*, 990–996; b) T. Ido, C.-N. Wan, V. Casella, J. S. Fowler, A. P. Wolf, *J. Labelled-Compd. Radiopharm.* **1978**, *14*, 175–183; c) J. H. Greenberg, M. Reivich, A. Alavi, P. Hand, A. Rosenquist, W. Rintelmann, A. Stein, R. Tusa, R. Dann, D. Christman, J. Fowler, B. MacGregor, A. Wolf, *Science* **1981**, *212*, 678–680; d) J. S. Fowler, A. P. Wolf, *Appl. Radiat. Isot.* **1986**, *37*, 663–668; e) P. Rigo, P. Paulus, B. J. Kaschten, R. Hustinx, T. Bury, G. Jerusalem, T. Benoit, J. Foidart-Willems, *Eur. J. Nucl. Med.* **1996**, *23*, 1641–1674.
- [2] a) W. C. Eckelman, *Drug Discovery Today* **2003**, *8*, 404–410; b) A. M. J. Paans, *Drug Discovery Today* **2003**, *8*, 734; c) T. Jones, *Drug Discovery Today* **2003**, *8*, 734–735; d) E. O. Aboagye, P. M. Price, T. Jones, *Drug Discovery Today* **2001**, *6*, 293–302; e) Special Issue: PET and SPECT in Medication Development, *Drug Development Res.* **2003**, *59* (2).
- [3] Y. Murakami, H. Takamatsu, A. Noda, K. Osoda, R. Ichise, M. Tatum, K. Tabata, T. Sawamoto, S. Nishimura, *J. Nucl. Med.* **2004**, *45*, 1946–1949.
- [4] *Radiopharmaceuticals for Positron Emission Tomography: Methodological Aspects* (Eds.: G. Stöcklin, V. W. Pike), Kluwer Academic Publishers, Dordrecht, **1993**.
- [5] M. af Ugglas, E. Tóth-Pál, H. Beving, K.-Å. Pettersson, *Annales Universitatis Turkuensis Ser. D: Medical Application of Cyclotrons* **1977**, *8*, 79–84.
- [6] a) G. W. Kabalka, R. M. Lambrecht, M. Sajjad, J. S. Fowler, S. A. Kunda, G. W. McCollum, R. MacGregor, *Int. J. Radiat. Isot.* **1985**, *36*, 853–855; b) M. S. Berridge, M. P. Franceschini, T. J. Tewson, K. L. Gould, *J. Nucl. Med.* **1986**, *27*, 834–837; c) M. S. Berridge, E. H. Cassidy, A. H. Terris, *J. Nucl. Med.* **1990**, *31*, 1727–1731.
- [7] J. F. Maddaluno, K. F. Faull, *Appl. Radiat. Isot.* **1990**, *41*, 873–878.
- [8] E. Nakamura, T. Inubushi, S. Aoki, D. Machii, *J. Am. Chem. Soc.* **1991**, *113*, 8980–8982.
- [9] M. Sawamura, Y. Kawaguchi, E. Nakamura, *Synlett* **1997**, 801–802.
- [10] A part of this work has been communicated: H. Yorimitsu, Y. Murakami, H. Takamatsu, S. Nishimura, E. Nakamura, *Angew. Chem.* **2005**, *117*, 2768–2771; *Angew. Chem. Int. Ed.* **2005**, *44*, 2708–2711.
- [11] Y. Yamamichi, N. Kaji, M. Fujiwara, Y. Minosako, A. Hayashi, Japan Kokai Tokkyo Koho, **1997**, JP09176179.
- [12] P. L. Durette, *Synthesis* **1980**, 1037–1038.
- [13] a) S. Nishimura, K. Yajima, N. Harada, Y. Ogawa, N. Hayashi, *J. Autom. Chem.* **1994**, *16*, 195–204; b) Y. Murakami, A. Kuroda, K. Osoda, S. Nishimura, *Tetrahedron Lett.* **2003**, *44*, 641–644.
- [14] a) E. P. Wesseler, R. Iltis, L. C. Clark, Jr., *J. Fluorine Chem.* **1977**, *9*, 137–146; b) J. G. Riess, M. Le Blanc, *Pure Appl. Chem.* **1982**, *54*, 2383–2406; c) *Oxygen and Ozone, Solubility Data Series, Vol. 7* (Ed.: R. Battino), Pergamon Press, New York, **1981**.
- [15] A. Ogawa, D. P. Curran, *J. Org. Chem.* **1997**, *62*, 450–451.
- [16] J. L. Brokenshire, K. U. Ingold, *Int. J. Chem. Kinet.* **1971**, *3*, 343–357.
- [17] a) H. Uchida, T. Okamoto, T. Ohmura, K. Shimizu, N. Satoh, T. Koike, T. Yamashita, *Nucl. Instrum. Methods Phys. Res. Sect. A* **2004**, *516*, 564–574; b) H. Takamatsu, T. Kakiuchi, A. Noda, H. Uchida, S. Nishiyama, R. Ichise, A. Iwashita, K. Mihara, S. Yamazaki, N. Matsuoka, H. Tsukuda, S. Nishimura, *Ann. Nucl. Med.* **2004**, *18*, 427–431.
- [18] A. Noda, The 44th Annual Meeting of the Japanese Society of Nuclear Medicine, Nov. 4–6, **2004**, Kyoto, 2VI333.
- [19] R. R. MacGregor, J. S. Fowler, A. P. Wolf, C.-Y. Shiue, R. E. Lade, C.-N. Wan, *J. Nucl. Med.* **1981**, *22*, 800–803.
- [20] M. Suzuki, R. Noyori, B. Långström, Y. Watanabe, *Bull. Chem. Soc. Jpn.* **2000**, *73*, 1053–1070.
- [21] B. Långström, T. Kihlberg, M. Bergström, G. Antoni, M. Björkman, B. H. Forngren, T. Forngren, P. Hartvig, K. Markides, U. Yngve, M. Ögren, *Acta Chim. Scandinavica* **1999**, *53*, 651–669.
- [22] W. C. Still, M. Kahn, A. Mitra, *J. Org. Chem.* **1978**, *43*, 2923–2925.
- [23] W. R. Roush, R. J. Brown, *J. Org. Chem.* **1983**, *48*, 5093–5101.
- [24] a) K. Hamacher, H. H. Coenen, G. Stöcklin, *J. Nucl. Med.* **1986**, *27*, 235–238; b) T. Chaly, J. R. Dahl, *Nucl. Med. Biol.* **1989**, *16*, 385–387; c) S. M. Moerlein, J. W. Brodack, B. A. Siegel, M. J. Welch, *Appl. Radiat. Isot.* **1989**, *40*, 741–743.

Received: August 15, 2006

Published online: December 5, 2006